Low-energy electron scattering with the purine bases of DNA/RNA using the R-matrix method

Amar Dora, Lilianna Bryjko, Tanja van Mourik, and Jonathan Tennyson

Citation: The Journal of Chemical Physics **136**, 024324 (2012); doi: 10.1063/1.3675448
View online: http://dx.doi.org/10.1063/1.3675448
View Table of Contents: http://scitation.aip.org/content/aip/journal/jcp/136/2?ver=pdfcov
Published by the AIP Publishing

Low-energy electron scattering with the purine bases of DNA/RNA using the R-matrix method

Amar Dora,[1,a)] Lilianna Bryjko,[2] Tanja van Mourik,[2] and Jonathan Tennyson[1,b)]
[1]*Department of Physics and Astronomy, University College London, Gower St., London WC1E 6BT, United Kingdom*
[2]*School of Chemistry, University of St Andrews, North Haugh, St. Andrews, Fife KY16 9ST, United Kingdom*

(Received 31 July 2011; accepted 15 December 2011; published online 13 January 2012)

R-matrix calculations on electron collisions with the purine bases found in DNA and RNA (i.e., adenine and guanine) are presented. Resonant anion states of these systems are identified by employing different approximation levels of *ab initio* theoretical methods, such as the static exchange, the static exchange plus polarization, and the close-coupling methods. The results are compared with other available calculations and experiments. All of these *ab initio* approximations, which we refer to as a scattering "model," give four shape resonances of $^2A''$ (π) symmetry within the energy range of 10 eV for both molecules. For adenine, the most sophisticated method, the close-coupling model, gives two very narrow $^2A'$ (σ) symmetry Feshbach-type resonances at energies above 5 eV. Quantitative results for the total elastic and electronic excitation cross sections are also presented. [doi:10.1063/1.3675448]

I. INTRODUCTION

With the realization that low-energy (sub 20 eV) electrons are produced abundantly in radiation tracks and are responsible for strand breaks in DNA,[1] there has been considerable interest in studying these low-energy electron collisions for their potential uses in medicine and to aid models of such processes. Experimental studies[2–12] have mostly concentrated on dissociative attachment (DA) by measuring production of anionic fragments of various constituents of DNA/RNA. However, there have also been experimental studies[3,7] using electron transmission spectroscopy (ETS) for measurement of electron attachment energies to the DNA bases in the gas phase, which aim to identify intermediary species responsible for the DA peaks observed in the experiments. The DNA bases (adenine, guanine, cytosine, and thymine) have low-lying unoccupied π-type molecular orbitals arising from the aromatic rings and are theorized to capture low-energy electrons to form temporary anions. These temporary anions (or resonant states of anions) are thought to provide the mechanism for strand breaks in DNA by transfer of excess energy to the sugar-phosphate backbone. Therefore, many of the current studies that aim to understand these processes focus on identifying and characterizing the resonances. This area has recently been the subject of a comprehensive review.[13]

A growing number of theoretical studies aiming to identify the resonant states in electron scattering with various DNA/RNA constituents and other related molecules have been performed. Specifically, calculations on phosphoric acid[14–16] and tetrahydrofuran,[16–18] as models for the phosphate and pentose sugar moieties that together make the DNA/RNA backbone, and even on the amino acid glycine[19] have been reported. However, as mentioned above, because of their favorable electron attachment centers, the nucleic acid bases in particular have been studied using several different theoretical methods.[20–27]

Shape resonances, which are formed by temporary occupation of electrons in low-lying empty molecular orbitals, can generally be characterized using relatively straightforward models (for example, see Refs. 25, 27, and 28). On the other hand, the description of Feshbach resonances, which are associated with electronically excited parent target states and are important, from an energetic point of view, for electron-impact dissociation, require more sophisticated models. Calculations employing such models are not possible with all scattering codes available. However, appropriate models for characterizing Feshbach resonances are implemented in the UK molecular **R**-matrix codes,[29] which allow for the inclusion of excited target states in the (close-coupling) expansion of the scattering wavefunctions. In our previous calculations on uracil[23] and H_3PO_4 (Ref. 14), we identified resonance states of Feshbach type; these were all found to lie at energies above 7 eV. The interesting problem of analyzing dissociation pathways of the resonant states and their role in the observed DNA strand breaks has been addressed in Ref. 30 and is not considered here. The main purpose of this work is to study electron collisions at a level beyond the static exchange and static exchange with polarization levels. To this end, we employ close-coupling calculations including excited target states represented at a partially correlated level.

In the present work, we report **R**-matrix calculations for electron scattering by the purine bases (adenine and guanine) using various models to identify their low-lying anionic resonant states. The total cross sections for elastic collisions as well as the electron impact excitations are also reported. Our previous work on low-energy electron scattering with uracil[23] reported on extensive tests of various parameters (such as the basis sets, numbers and types of valence and virtual molecular orbitals, and **R**-matrix sphere size) at all levels of target

[a)]Present address: Laboratoire Aime Cotton du CNRS, Universite de Paris-Sud, 91405 Orsay, France.
[b)]Electronic mail: j.tennyson@ucl.ac.uk.

and scattering calculations. Therefore, in the present paper, we only report limited tests of such factors and concentrate on the effects of polarization introduced by various *ab initio* approximate models on the resonance parameters.

II. THEORY

The **R**-matrix method is based upon the separation of space into two regions by considering the nature of the interactions between the scattering electron and the target system. This is achieved by enclosing the target inside an imaginary sphere large enough to contain the entire N-electron target wavefunction. Outside this sphere, the electron and the target can be described by their long-range multipolar interactions. Inside the sphere, the description of the $(N + 1)$-electronic wavefunction of the electron + target system must take care of the exchange and correlation effects among all the $N + 1$ electrons. Inside the sphere, this $(N + 1)$-electronic wavefunction ψ_k^{N+1} is expressed as a close-coupling (CC) expansion,

$$\psi_k^{N+1} = \mathcal{A} \sum_{ij} a_{ijk} \Phi_i^N(\mathbf{x}_1, \ldots, \mathbf{x}_N) u_{ij}(\mathbf{x}_{N+1}) + \sum_i b_{ik} \chi_i^{N+1}(\mathbf{x}_1, \ldots, \mathbf{x}_{N+1}), \quad (1)$$

where, in the first summation, Φ_i^N is the wavefunction of the ith target state, u_{ij} are the continuum orbitals to represent the scattering electron, and $\mathcal{A}$ is the anti-symmetrization operator. The χ_i^{N+1}, in the second term, are the so-called L^2 configurations, which have zero amplitude at the spherical boundary. These L^2 configurations are created by placing all the N+1 electrons into the molecular orbitals (MOs) associated with the target and are essential in even the simplest model employed (static exchange, see below), as they allow for relaxation of the enforced orthogonalization between the continuum orbitals and the target orbitals. Indeed, allowing the scattering electron to enter unoccupied target MOs included in the calculation is essential for completeness and to model high-ℓ effects in the region of the target nuclei. In more sophisticated models, as will be discussed below, the L^2 configurations also help model the effects of target polarization in response to the scattering electron. The a_{ijk} and b_{ik} in Eq. (1) are the variational coefficients obtained by diagonalizing the N + 1 Hamiltonian inside the sphere. The diagonalization of this inner-region Hamiltonian can be very demanding depending on the type of the expansion we choose for ψ_k^{N+1} in Eq. (1).

A major advantage of the **R**-matrix method is that the inner-region Hamiltonian is independent of the scattering energy and solved only once. The energy dependence of the scattering calculation comes while solving the outer-region problem, which is computationally cheap. For more details on the theory and its implementation in the UK molecular **R**-matrix codes, the reader is referred to the recent review article by one of us.[31] Below, we just mention aspects that are relevant from the point of view of the present work.

With the UK molecular **R**-matrix codes,[29] different scattering models can be constructed by choosing different types of expansion for the target and the corresponding L^2 configurations in Eq. (1). In this work, we use three different models: static exchange (SE), SE plus polarization (SEP), and the close-coupling (CC) models. The SE and SEP models are among the simplest standard electron-molecule scattering approximations, which are also used in other theoretical methods; for example, the Schwinger multi-channel (SMC) calculations by Winstead and McKoy used these models to study electron collisions with the purine bases.[22] We compare with these results below.

In both SE and SEP models, the target MOs used are obtained from Hartree-Fock (HF) self-consistent-field (SCF) calculations and the target is represented by the HF ground-state wavefunction. In the SE model, the L^2 configurations are obtained by the occupation of the (N + 1)th electron to the low-lying target virtual MOs. In the SEP model, the above set of L^2 configurations is augmented with those arising from the occupation of both the (N + 1)th electron and any single excited electron from the target valence occupied MOs to the virtual MOs. These latter configurations are added to represent the target polarization effects in presence of the scattering electron. By this construction, the SE model is only capable of describing shape resonances and places the resonances at higher energies in comparison with the SEP and CC models. However, the SE model is a well-defined approximation without artificial problems such as the occurrence of pseudo-resonances, and thus helpful in cross-comparison with other theoretical methods and models. We note that pseudo-resonances are non-physical resonances encountered in any method that treats the polarization effect and does not explicitly include the channels that would otherwise be open in the energy range considered.

Our best results are obtained with the CC model, in which several target states are used in the first sum of Eq. (1). With the explicit use of the parent excited target states in the CC expansion, the CC model is capable of treating Feshbach resonances and can also calculate electron impact excitation cross sections. In this study, we use the recommended[32] complete active space (CAS) configuration interaction (CI) method to represent the target states in the CC calculations. In the CAS-CI method, all possible configurations (only restricted by the space-spin symmetry of the problem) resulting from the distribution of a set of active electrons among a set of valence MOs are taken into account. Therefore, the target electronic states are represented at a partially correlated level. To obtain the L^2 configurations for the CC model, the extra electron is added to this set of active electrons; this ensures a good balance of electron-electron correlation between the target and the scattering calculation in the CC model. A standard CC calculation involves contraction of configurations arising from placing the scattering electron into the virtual and scattering orbitals,[32] i.e., including the virtual orbitals as part of the first sum in Eq. (1). This contracted CC method produces a smaller number of configuration state functions (CSFs) for a selected CAS-CI model and is, therefore, computationally cheaper. However, this method has proved to be extremely slowly convergent with respect to the number of target states included[23,33] and tends to overestimate resonance positions unless exceptionally large and systematically chosen CC expansions are used. Not contracting the virtual orbitals, in other words, including them in the second sum in Eq. (1),

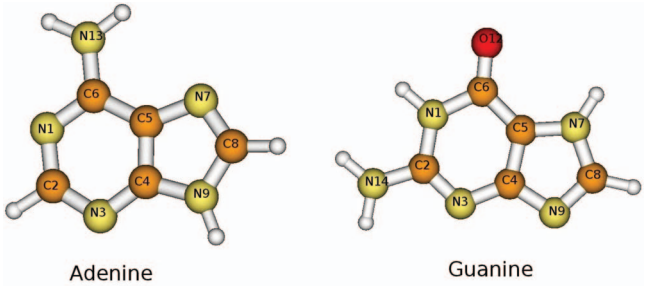

FIG. 1. The structures of N9H-adenine and keto-N7H-guanine considered in this work (drawn with GAUSSVIEW 4.1.2).

produces a much larger number of CSFs, which leads to extra correlation in the scattering calculation and, thus, systematically lowers resonance positions. However, it is not clear that this uncontracted CC approach, which we refer to as the u-CC model, is completely balanced.[32]

III. CALCULATIONS

A. Target models

Adenine and guanine can exist in different tautomeric forms depending on their environment. In this study, we used the N9H-adenine and keto-N7H-guanine tautomers.[34] The nuclear geometry optimization calculations for these tautomers were done using the B3LYP method and the 6-31+G* basis set employing the GAUSSIAN 03 package.[35] The optimized geometries of both molecules revealed that they have nearly planar structures.[36] Therefore, to take advantage of the computational and analytical simplifications offered in case of planar molecular symmetry, the geometry optimizations were redone restricting the molecules to their planar geometries. The resulting planar structures of both molecules are shown in Fig. 1. In passing we note that the optimized nonplanar adenine molecule possesses only a very slightly lower energy and slightly larger dipole moment (−467.339875 E_h, 2.50 D) than its planar counterpart (−467.339857 E_h, 2.46 D). For guanine, the optimized nonplanar structure has lower energy and dipole moment (−542.577446 E_h, 1.80 D) compared to the planar structure (−542.576074 E_h, 2.22 D). With the planar C_s symmetry of the molecules, the ground state electronic configuration of adenine is $(1a' - 29a')^{58}(1a'' - 6a'')^{12}$ and that of guanine is $(1a' - 32a')^{64}(1a'' - 7a'')^{14}$.

For the representation of target electronic states in the **R**-matrix calculation, several basis sets (such as cc-pVDZ, aug-cc-pVDZ, and cc-pVTZ) were initially tried. However, in order to keep the computationally demanding scattering calculations tractable, the cc-pVDZ was finally adopted. Therefore, unless otherwise stated, all reported results used the cc-pVDZ basis set for the target.

In the SE and SEP models, the target is represented at the HF level. The occupied MOs and unoccupied virtual MOs were obtained from the SCF calculations. Here, no attempt was made to calculate or use modified virtual orbitals (MVOs) as suggested by Winstead and McKoy[21,22], because in our previous calculations on uracil[23] the use of MVOs did not yield any significant improvement in the results. The SCF ground state energy and dipole moment for adenine are −464.558845 a.u. and 2.41 D, respectively, while the corresponding values for guanine are −539.437628 a.u. and 2.10 D, respectively.

For the CC model, the target states are represented at the CAS-CI level. The target orbitals are obtained from the state-averaged CASSCF (SA-CASSCF) calculations. Several CASSCF calculations with different active spaces and different number of states were performed. Ideally, the active space for conjugated molecular systems should contain all valence π-orbitals and all lone-pair orbitals. But such a selection of active space would result in a massive increase of computational cost in the corresponding scattering calculations. Initially, we employed for adenine an active space of 14 valence electrons in 12 orbitals of the configuration type $(1a' - 28a')^{56}$, $(29a' - 30a', 1a'' - 10a'')^{14}$, which gave a ground-state energy of −464.651785 E_h and dipole moment of 2.75 D with the cc-pVDZ basis set. But, this calculation led to a CC calculation that is unmanageable at present. We, therefore, had to restrict the CASSCF calculation to a manageable 14 electrons distributed over 10 orbitals (i.e., the CASSCF(14,10) model) represented by $(1a' - 28a')^{56}$, $(29a' - 30a', 1a'' - 8a'')^{14}$. For similar computational reasons, we had to use a restricted active space of CASSCF(12,9) in the calculations on guanine with the first three a'' MOs frozen, i.e., the $(1a' - 30a', 1a'' - 3a'')^{66}$, $(31a' - 32a', 4a'' - 10a'')^{12}$ configuration.

The number of states included in the SA-CASSCF calculation also had an effect on the convergence of the selected CASSCF calculation. We found that, for adenine, 20 states (i.e., five states from each space-spin symmetry) and, for guanine, 16 states (i.e., four states from each space-spin symmetry) gave convergence for the selected CASSCF models. Therefore, in the CC calculations, we used a 20-state expansion for adenine and a 16-state expansion for guanine. Table I contains the CASSCF ground state energy, vertical excitation energies, and ground-state dipole moments of adenine and guanine, calculated with the cc-pVDZ and cc-pVTZ basis sets. All SCF and CASSCF calculations were performed with the MOLPRO 2006.1 (Ref. 37) computational package. Other computational estimates of the excitation energies of different tautomers of adenine and guanine have been reported in the literature. These include semi-empirical calculations[38] of the adiabatic excitation energies, and CASSCF and CASPT2 calculations[39] of the vertical excitation energies. The CASSCF and CASPT2 vertical excitation energies from Ref. 39 are included in Table I for the sake of comparison. Their CASSCF values agree very well with our results; the small differences between the CASSCF excitation energies of Ref. 39 and our results can be attributed to the use of different active spaces and basis sets. For the experimentally observed absorption bands of the purine bases in the gas phase or aqueous solution and for their assignments, we refer the interested reader to Refs. 39 and 40, and the references therein.

B. Scattering models

All scattering calculations reported here used an **R**-matrix sphere of radius $a = 13\,a_0$. **R**-matrix sphere sizes

TABLE I. The CASSCF $X\,^1A'$ ground state energies (in E_h), the vertical excitation energies (in eV), and the ground state dipole moments (in D) of adenine and guanine. The CASSCF and CASPT2 vertical excitation energies from Ref. 39 are included for comparison.

	Adenine				Guanine			
State	cc-pVDZ	cc-pVTZ	CASSCF	CASPT2	cc-pVDZ	cc-pVTZ	CASSCF	CASPT2
X^1A'	−464.59272	−464.70968			−539.47665	−539.62022		
$2^1A'$	6.09	6.05	5.73	5.13	6.07	6.01	6.08	4.76
$3^1A'$	6.93	6.85	6.48	5.20	6.58	6.52	6.99	5.09
$4^1A'$	8.37	8.29	7.80	6.24	8.14	8.16	7.89	5.96
$5^1A'$	9.08	9.01						
$1\,^1A''$	6.86	6.83	6.43	6.15	5.66	5.94	6.22	5.79
$2\,^1A''$	7.10	7.08	7.16	6.86	7.11	7.07	8.05	6.60
$3\,^1A''$	8.04	7.31			7.98	7.86	7.97	6.63
$4\,^1A''$	8.52	7.93			8.14	8.35	8.99	7.16
$5\,^1A''$	10.01	9.38						
$1\,^3A'$	4.51	4.47			3.93	3.88		
$2\,^3A'$	5.88	5.83			5.02	5.06		
$3\,^3A'$	6.09	6.08			5.75	5.74		
$4\,^3A'$	6.75	6.66			7.14	7.17		
$5\,^3A'$	8.75	8.70						
$1\,^3A''$	6.47	6.46			5.53	5.83		
$2\,^3A''$	6.85	6.81			6.85	6.81		
$3\,^3A''$	7.98	7.28			7.84	7.68		
$4\,^3A''$	8.31	7.78			8.12	8.33		
$5\,^3A''$	9.91	9.29						
$\mu(X\,^1A')$	3.00	3.06			1.58	1.35		

smaller than this were not tested as they are likely to be too small to confine the target wavefunction; test calculations with $a = 15\,a_0$ gave similar results to those at $a = 13\,a_0$. The continuum orbitals, appropriate for the given size of sphere, are used to represent the scattering electron and are expanded in a basis of Gaussian-type functions centered on the center of mass of the target by using $\ell \leq 4$ partial waves in a procedure as described by Faure *et al.*[41] The long-range scattering, dominated by interaction of higher partial waves ($\ell > 4$) with the molecular dipole potential, are taken into account by using the Born approximation[42] at a later stage, outside the **R**-matrix calculations. The continuum orbitals were first symmetrically orthogonalized among themselves. Only those combinations of continuum orbitals with an eigenvalue greater than 10^{-7} in the symmetric orthogonalization of the overlap matrix ($\langle u_{ij}|u_{i'j'}\rangle$) were retained in order to avoid linear dependence problems. The retained continuum orbitals were subsequently Schmidt orthogonalized to the target MOs. Based on experience with previous **R**-matrix calculations,[14,23] the number of target virtual orbitals retained in the calculations is crucial for getting the correct number of resonances and their positions. Here, 15 virtual orbitals were used for each symmetry for all models.

In the case of our uncontracted CC (u-CC) calculation for uracil[23] with 15 virtual orbitals, we obtained satisfactory resonance positions that were close to the experimentally observed values.[3] In the current calculations for adenine and guanine, we followed the same approach. Thus, our final and best results are obtained by the uncontracted CC method using 15 virtual orbitals. This model produced a large number of CSFs, i.e., 181 454 A'' and 181 266 A' CSFs for adenine, and 91 018 A'' and 90948 A' CSFs for guanine. To deal with the diagonalization of such large Hamiltonian matrices, we make use of the partitioned **R**-matrix method,[43] which requires only a small proportion (significantly less than 10%) of the eigensolutions of the full scattering Hamiltonian. In this study, we used the lowest 5000 eigensolutions for the uncontracted CC calculations; this choice typically took around 10 days to finish the calculation for each symmetry on a 64-bit, 4-core workstation using a parallel version of the code optimized for this task.[44]

In solving the outer-region problem, the scattering eigenphase sums and cross sections are evaluated. Fitting the resulting eigenphase sums to a Breit-Wigner formula gives the positions and widths of the resonances. This fitting of the eigenphase sums to Breit-Wigner profiles is performed automatically by a module called RESON (Ref. 45) in the UK **R**-matrix codes.

For molecules with permanent dipole moments, such as the ones considered here, the partial wave expansion does not converge in the fixed-nuclei approximation. It is important to include the effects of partial waves higher than $\ell = 4$ as they have a profound effect on the total elastic cross section at low energy. Corrections were computed directly for the cross sections using the Born approximation method of Chu and Dalgarno[42] as implemented in the routine BORNCROSS.[46] This treatment also includes the effects of target rotational motion, which acts to average out the effects of the asymptotic dipole potential. At low energies, the elastic cross sections scale approximately with the square of the target permanent dipole moment; as our calculated target models give reasonable values for these dipoles, we can

TABLE II. Positions (and widths) of low-lying A'' (or π) shape resonances computed using different models with the cc-pVDZ basis set for adenine and guanine. All quantities are in eV.

Bases	Models	$A''(\pi)$-resonances			
Adenine	SE	3.23 (0.53)	4.02 (0.33)	5.06 (1.11)	10.62 (0.40)
	SEP	1.30 (0.14)	2.12 (0.09)	3.12 (0.28)	7.07 (0.24)
	CC	2.38 (0.36)	3.35 (0.23)	4.78 (0.89)	7.54 (1.44)
	u-CC	1.58 (0.22)	2.44 (0.14)	4.38 (0.67)	7.94 (0.57)
	Ref. 25	2.40 (0.20)	3.20 (0.20)	4.40 (0.30)	9.00 (0.50)
	Refs. 20 and 22	1.10	1.80	4.10	
	Obs. [3]	0.54	1.36	2.17	
Guanine	SE	3.00 (0.33)	4.47 (0.35)	5.66 (0.80)	10.12 (1.26)
	SEP	1.83 (0.16)	3.30 (0.24)	4.25 (0.33)	7.36 (0.27)
	CC	1.68 (0.13)	3.19 (0.21)	4.74 (0.43)	6.96 (0.42)
	u-CC	0.97 (0.006)	2.41 (0.15)	3.78 (0.29)	6.41 (0.72)
	Ref. 25	2.40 (0.20)	3.80 (0.25)	4.80 (0.35)	8.90 (0.60)
	Refs. 20 and 22	1.55	2.40	3.75	
	Obs.[3]	0.46	1.37	2.36	

expect that the low-energy elastic cross sections should be realistic.

IV. RESULTS AND DISCUSSION

A. Adenine

Using all four models, we find at least four low-energy shape resonances of $^2A''$ symmetry for adenine. This finding was checked at the SE and SEP level by repeating the calculation with a cc-pVTZ target basis; the resonance parameters were stable to this change. Table II compares the positions and widths of these resonances with other available calculated and experimental estimates. In all of these models, the first three resonances form an approximate and closely spaced series with the resonances separated by approximately 1 eV. This is in accordance with the observed data.[3] The fourth resonance appears at higher energy and seems to have been missed by the experiment. Our SE model places the resonances at too high energies as expected; the positions are in quantitative agreement with the SE calculations of Winstead and McKoy[22] who used the SMC method but did not provide their exact resonance positions. This similarity is expected as both the *ab initio* methods use the standard SE potential; any minor differences will be due to the differences in the geometries and basis set, etc. The **R**-matrix calculation of Tonzani and Greene,[25] which uses a one-electron scattering model employing simple local approximations to the exchange and polarization effects, gives resonance positions 0.7–1.6 eV lower than our SE results (i.e., at 2.4, 3.2, 4.4, and 9.0 eV).

The polarization effect included in the SEP model brings down the resonance positions towards the observed values,[3] but are still about 1 eV higher than these. The SEP calculations of Winstead and McKoy give resonance positions that are in good agreement with our first two resonances, but the value of their third resonance position is 1 eV higher than ours.

The effect of resonances on the elastic cross sections can be seen in Fig. 2, which is plotted separately for $^2A'$ and $^2A''$ symmetries for all models employed. The presence of resonances of $^2A'$ symmetry has not been reported in any previous works on adenine. In our $^2A'$ calculations, we find resonant features in all of our models although they appear at higher energies, above 5 eV. The resonant features can be seen in the eigenphase sum and the cross section plots (see Fig. 2). The SE calculation finds two shape resonances, one at 9.85 eV (width 0.59 eV) and another at 10.60 eV (width 0.63 eV). The CC calculation puts the resonances at 7.82 eV (width 0.17 eV) and 8.69 eV (width 0.61 eV). Both the SEP and the uncontracted CC calculations show very narrow structures with characteristics of Feshbach resonances. These types of narrow Feshbach resonances were also seen in our previous studies on uracil (Ref. 23) and H_3PO_4 (Ref. 14) for the SEP and CC calculations. The first Feshbach resonance in our uncontracted CC calculation comes at 5.82 eV (width 0.0095 eV) and another close-by at 6.05 eV (width 0.0038 eV). These two resonances appear to be associated with the parent target states at 5.88 eV ($2\,^3A'$) and 6.09 eV ($2\,^1A'$ and $3\,^3A'$) (see Table I), respectively, although we note that identifying resonances with a single parent state is not always possible, even for very simple systems.[47]

The total elastic cross section for electron collisions with the adenine molecule is presented in Fig. 3 for our final uncontracted CC calculation. The cross section increases rapidly at lower energies, which is expected for polar molecules. We add a Born correction to compensate for the truncation of the partial wave expansion in the calculation in this polar molecule. This huge correction almost washes out the peaks due to the resonances. To the best of our knowledge, there have been no measurements on total elastic cross section to compare with.

Figure 4 presents our calculated electron impact electronic excitation cross sections. Only excitations to the first two triplet and singlet states of A' symmetry are shown. The cross sections for other excitations are found to be very small; as can be seen, even the values shown are fairly small. For excitations to the singlet states, we have added the Born corrections. To compute these, we used transition dipole moments of 0.41 a.u. (for $2\,^1A'$) and 1.50 a.u. (for $3\,^1A'$) as calculated

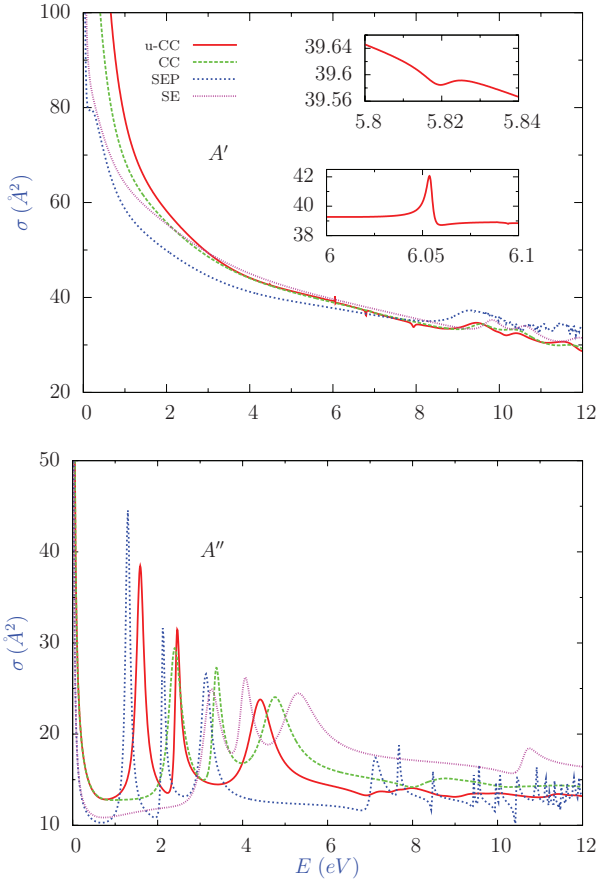

FIG. 2. Elastic cross sections of electron collision with adenine. Contributions from the A' and A'' symmetry are shown separately to identify the resonances in different models. The insets illustrate the effect of the Feshbach resonance for the uncontracted close-coupling (u-CC) model only.

using MOLPRO. As seen in Fig. 4, excitation to the first $^1A'$ state shows a sharp peak at 6.8 eV. This peak comes entirely from the $^2A'$ resonance, while the large peak at 7.0 eV for excitation to the first $^3A'$ state is exclusively due to the $^2A''$ resonance. As far as we know, there have been no other calculations or measurements on electronic excitation cross sections.

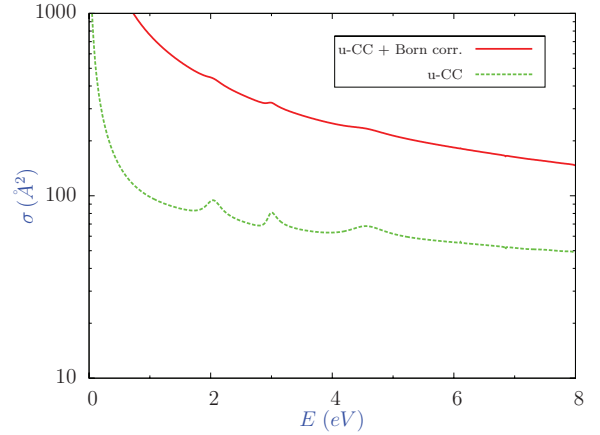

FIG. 3. Total elastic cross section for low-energy electron collisions with adenine in the final uncontracted CC model (with and without the Born correction).

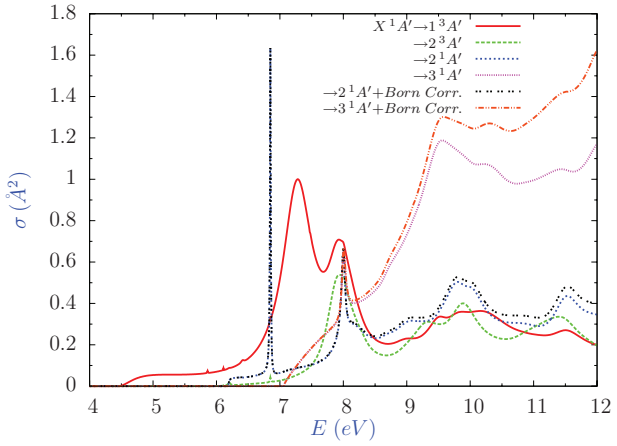

FIG. 4. Electron impact excitation cross sections of adenine to the lowest two singlet and triplet A' states. For the singlet states, the Born contribution is shown. The excitation cross sections to the A'' states were very small.

B. Guanine

As in the case of adenine, all our models find four $^2A''$ shape resonances below 10 eV for guanine. The resonance parameters are presented in comparison with other available calculations and the ETS measurements of Aflatooni *et al.*[3] in Table II. As can be seen in Table II, the observed resonances by Aflatooni *et al.* appear at almost the same positions for adenine and guanine; this similarity of resonance positions in the purine bases is also reflected in most of our models. Our CC calculations give better results for guanine than for adenine; in particular, the uncontracted CC model gives resonance positions close to those observed values. For adenine, we found that freezing the highest occupied MO of a' symmetry increased the lowest two resonance positions by ∼0.5 eV in the u-CC model, while the target excitation energies remained approximately the same. Therefore, inclusion of more occupied a' orbitals into the active space (or at least including the highest two occupied a' orbitals into the active space, as done for guanine) may decrease the resonance positions. Other factors, such as the inclusion of more virtual MOs in the calculations, may have similar effects on the results. However, as mentioned above, scattering calculations with larger CASSCF configurations than used here are unmanageable at this stage.

The presence of resonances of $^2A'$ symmetry is less clear in our calculations on guanine. The SE calculation shows two shape resonances below 10 eV; one at 8.58 eV (width 0.21 eV) and the other at 9.83 eV (width 0.39 eV), while the CC calculation finds them at 6.44 eV (width 0.97 eV) and 7.49 eV (width 1.72 eV). In the uncontracted CC calculation, the lowest two resonances appear at 6.04 eV (width 1.23 eV) and 7.01 eV (width 0.49 eV). Again, there are no other works on this to compare our results with.

Figure 5 shows elastic electron collision cross sections for guanine, separately for the $^2A'$ and $^2A''$ symmetries, for all models employed to aid identifying the role of resonances in the cross sections. Figure 6 presents the total elastic cross section for the final uncontracted CC calculation and the total elastic cross section augmented with the Born correction. The

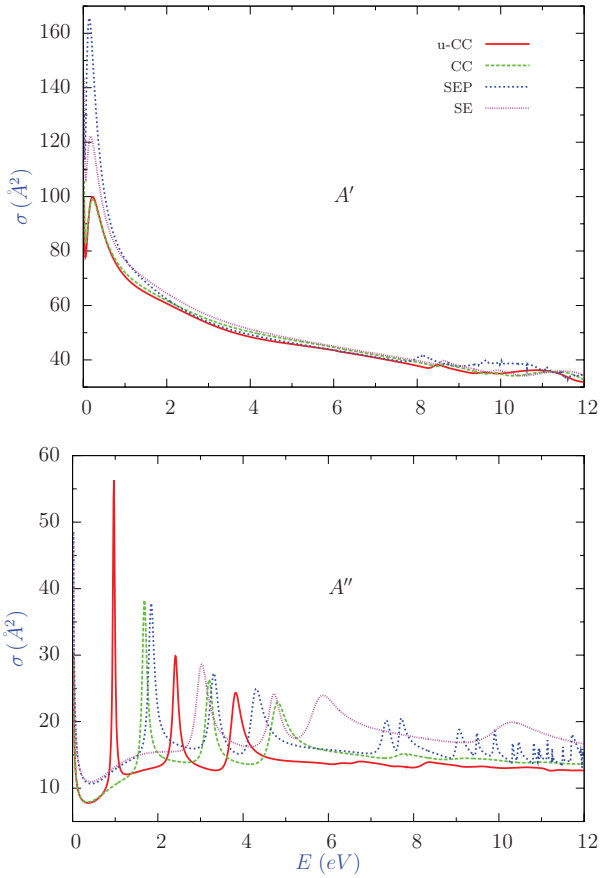

FIG. 5. Elastic cross sections of electron collision with guanine. The contributions from the A' and A'' symmetry are shown separately to identify the resonances.

dipole moment of guanine is almost half in size compared to that of adenine, which results in a much smaller Born correction.

Figure 7 presents the calculated electron impact electronic excitation cross sections for guanine. Here, we show excitations to the first three triplet and first two singlet A' states. The excitations to the A'' states were found to be very

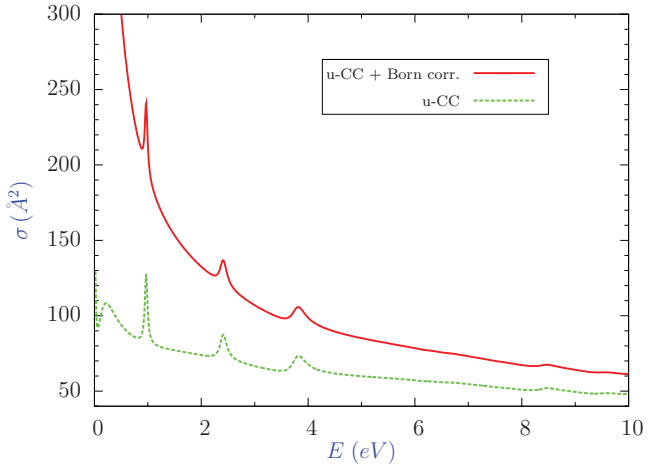

FIG. 6. Total elastic cross section for low-energy electron collisions with guanine in the final uncontracted CC model (with and without the Born correction).

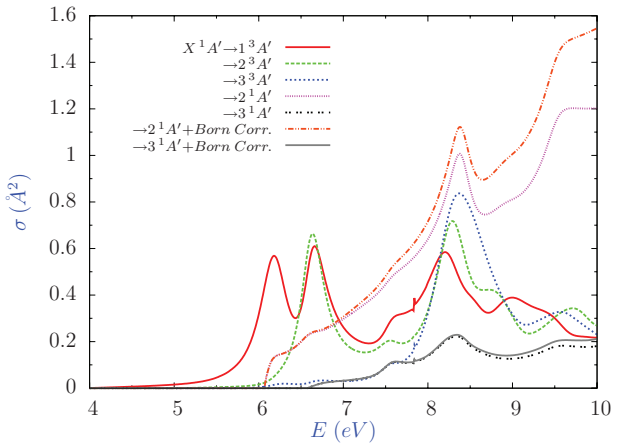

FIG. 7. Electron impact excitation cross section of guanine to the lowest two singlet and three triplet A' states. For the singlet states, the Born contribution is shown. The other excitation cross sections were very small.

small. For excitations to the singlet states, the Born corrections have been added and are also shown separately in this figure. The transition dipole moment values, used for the calculation of the Born corrections, are found to be 1.26 a.u. for $2\,^1A'$ and 0.49 a.u. for $3\,^1A'$. The excitation cross sections to the triplet states are dominated by the $^2A''$ resonance and those to the singlet states mostly by the $^2A'$ resonance.

V. CONCLUSION

Calculations are presented for electron collision with adenine and guanine using different scattering models. For both bases, four shape resonances of $^2A''$ symmetry were found, which fall almost within the same energy range below 10 eV for adenine, $^2A'$ symmetry resonances of Feshbach character have been identified for the first time. These are found to lie above 5 eV and have very narrow widths. The role of Feshbach-type resonances has particular significance from the point of view of dissociation. They have larger lifetimes than shape resonances and can decay back to the excited states.

The discrepancies between our calculated results and the experimental positions may arise in part due to the planar restrictions on geometry in our calculations. As has also been noted by Winstead and McKoy,[22] the experiment on guanine in fact employed the enol tautomer, which is the most stable form of guanine in the gas phase. Here, we study the keto form as found in DNA/RNA. One other possible factor contributing to the discrepancy is our limited treatment of polarization effects. In particular, the active space we were able to use for adenine may well have been insufficient explaining the worse results for this system. The complete *ab initio* treatment of polarization effects is crucial in getting correct resonance parameters and is computationally very demanding. The molecular **R**-matrix with pseudo-states (RMPS) method[48,49] has been demonstrated to systematically improve the polarization effects.[50,51] However, at present it is computationally too expensive to perform RMPS calculations for molecules of the size considered here. Indeed, the calculations presented in this work constitute the limit that could be achieved at this time.

ACKNOWLEDGMENTS

This project was funded by the UK Engineering and Physical Sciences Research Council. L.B. and T.v.M. thank EaStCHEM for computational support via the EaStCHEM Research Computing Facility. A.D. was supported in part by the ANR (France) under Contract No. 09-BLAN-020901.

[1] B. Boudaïffa, P. Cloutier, D. Hunting, M. A. Huels, and L. Sanche, Science **287**, 1658 (2000).
[2] C. Desfrançois, H. Abdoul-Carime, and J. P. Schermann, J. Chem. Phys. **104**, 7792 (1996).
[3] K. Aflatooni, G. A. Gallup, and P. D. Burrow, J. Phys. Chem. A **102**, 6205 (1998).
[4] G. Hanel, B. Stir, S. Denifl, P. Scheier, M. Probst, B. Farizon, M. Farizon, E. Illenberger, and T. D. Märk, Phys. Rev. Lett. **90**, 188104 (2003).
[5] S. Denifl, S. Ptasińska, G. Hanel, B. Stir, M. Probst, P. Scheier, and T. D. Märk, J. Chem. Phys. **120**, 6557 (2003).
[6] S. Denifl, S. Ptasińska, G. Hanel, B. Stir, P. Scheier, M. Probst, B. Farizon, M. Farizon, S. Matejcik, E. Illenberger, and T. D. Märk, Phys. Scr., T **T110**, 252 (2004).
[7] A. M. Scheer, K. Aflatooni, G. A. Gallup, and P. D. Burrow, Phys. Rev. Lett. **92**, 068102 (2004).
[8] A. M. Scheer, C. Silvernail, J. A. Belot, K. Aflatooni, G. A. Gallup, and P. D. Burrow, Chem. Phys. Lett. **411**, 46 (2005).
[9] K. Aflatooni, A. M. Scheer, and P. D. Burrow, Chem. Phys. Lett. **408**, 426 (2005).
[10] R. Abouaf and H. Dunet, Eur. Phys. J. D. **35**, 405 (2005).
[11] P. D. Burrow, G. A. Gallup, A. M. Scheer, S. Denifl, S. Ptasińska, T. D. Märk, and P. Scheier, J. Chem. Phys. **124**, 124310 (2006).
[12] K. Aflatooni, A. M. Scheer, and P. D. Burrow, J. Chem. Phys. **125**, 045301 (2006).
[13] I. Baccarelli, I. Bald, F. A. Gianturco, E. Illenberger, and J. Kopyra, Phys. Rep. **508**, 1 (2011).
[14] L. Bryjko, T. van Mourik, A. Dora, and J. Tennyson, J. Phys. B **43**, 235203 (2010).
[15] C. Winstead and V. McKoy, Int. J. Mass Spectrom. **277**, 279 (2008).
[16] S. Tonzani and C. H. Greene, J. Chem. Phys. **125**, 094504 (2006).
[17] D. Bouchiha, J. D. Gorfinkiel, L. G. Caron, and L. Sanche, J. Phys. B **39**, 975 (2006).
[18] C. S. Trevisan, A. E. Orel, and T. N. Rescigno, J. Phys. B **39**, L255 (2006).
[19] M. Tashiro, J. Chem. Phys. **129**, 164308 (2008).
[20] C. Winstead and V. McKoy, Radiat. Phys. Chem. **77**, 1258 (2008).
[21] C. Winstead and V. McKoy, J. Chem. Phys. **125**, 174304 (2006).
[22] C. Winstead and V. McKoy, J. Chem. Phys. **125**, 244302 (2006).
[23] A. Dora, J. Tennyson, L. Bryjko, and T. van Mourik, J. Chem. Phys. **130**, 164307 (2009).
[24] C. Winstead and V. McKoy, J. Chem. Phys. **127**, 085105 (2007).
[25] S. Tonzani and C. H. Greene, J. Chem. Phys. **124**, 054312 (2006).
[26] F. A. Gianturco, F. Sebastianelli, R. R. Lucchese, I. Baccareli, and N. Sanna, J. Chem. Phys. **128**, 174302 (2008).
[27] Y.-F. Wang and S. X. Tian, Phys. Chem. Chem. Phys. **13**, 6169 (2011).
[28] J. Berdys, I. Anuszkiewicz, P. Skurski, and J. Simons, J. Am. Chem. Soc. **126**, 6441 (2004).
[29] L. A. Morgan, J. Tennyson, and C. J. Gillan, Comput. Phys. Commun. **114**, 120 (1998).
[30] R. Barrios, P. Skurski, and J. Simons, J. Phys. Chem. B. **106**, 7991 (2002).
[31] J. Tennyson, Phys. Rep. **491**, 29 (2010).
[32] J. Tennyson, J. Phys. B **29**, 6185 (1996).
[33] H. N. Varambhia and J. Tennyson, J. Phys. B **40**, 1211 (2007).
[34] W. Caminati, Angew. Chem. Int. Ed. **48**, 9030 (2009).
[35] M. J. Frisch, G. W. Trucks, H. B. Schlegel *et al.*, GAUSSIAN 03, Revision C.02, Gaussian, Inc., Wallingford, CT, 2004.
[36] J. Sponer and P. Hobza, J. Phys. Chem. **94**, 3161 (1994).
[37] H.-J. Werner, P. J. Knowles, F. R. Manby, M. Schütz *et al.*, MOLPRO, version 2006.1, a package of *ab initio* programs, 2006, see http://www.molpro.net.
[38] P. Mishra and K. Jug, J. Mol. Struct.: THEOCHEM **305**, 139 (1994).
[39] M. P. Fülscher, L. Serrano-Andrés, and B. O. Roos, J. Am. Chem. Soc. **119**, 6168 (1997).
[40] D. Varsano, R. D. Felice, M. A.L. Marques, and A. Rubio, J. Phys. Chem. B **110**, 7129 (2006).
[41] A. Faure, J. D. Gorfinkiel, L. A. Morgan, and J. Tennyson, Comput. Phys. Commun. **144**, 224 (2002).
[42] S.-I. Chu and A. Dalgarno, Phys. Rev. A **10**, 788 (1974).
[43] J. Tennyson, J. Phys. B **37**, 1061 (2004).
[44] R. Zhang, P. G. Galiatsatos, and J. Tennyson, J. Phys. B **44**, 195203 (2011).
[45] J. Tennyson and C. J. Noble, Compu. Phys. Commun. **33**, 421 (1984).
[46] K. L. Baluja, N. J. Mason, L. A. Morgan, and J. Tennyson, J. Phys. B **33**, L677 (2000).
[47] D. T. Stibbe and J. Tennyson, J. Phys. B **30**, L301 (1997).
[48] J. D. Gorfinkiel and J. Tennyson, J. Phys. B **37**, L343 (2004).
[49] J. D. Gorfinkiel and J. Tennyson, J. Phys. B **38**, 1607 (2005).
[50] M. Jones and J. Tennyson, J. Phys. B **43**, 045101 (2010).
[51] R. Zhang, K. L. Baluja, J. Franz, and J. Tennyson, J. Phys. B **44**, 035203 (2011).